

## Spectral and spatial atmospheric correction of Terra/MODIS remote sensing data

**U.M. Sultangazin**, A.Kh. Akhmedzhanov, V.N. Glushko, L.A. Egorova,  
T.K. Karadanov, P.G. Lysenko, and L.V. Shagarova

*Institute of Space Research, Central Astro-Physical Institute,  
Academy of Sciences of Kazakhstan Republic, Almaty*

Received June 13, 2006

Atmospheric correction of space images with the use of numerical matrices of radiation intensity values recorded by the Terra/MODIS satellite, as well as simultaneous ground measurements of optical characteristics of the atmosphere are under consideration.

The object of the study of natural resources of the Earth by means of spaceborne devices are the characteristics of solar radiation reflected from natural formations on the ground surface or characteristics of their own radiation. Solar and ground surface radiation is transformed when passing through the atmosphere, so it is necessary to take into account the effect of the atmosphere.

To retrieve different characteristics of the ground surface based on satellite observations in the visible wavelength range, atmospheric correction of space images is required in order to remove the distortions introduced by the atmosphere.

Significant theoretical results were obtained when solving the problem mathematically.<sup>1-11</sup> Different approaches are characterized by different degree of simplification of the composition and structure of the atmosphere, therefore, they are developed taking into account different variability of the atmospheric parameters and the variety of the types of the underlying surface.

In this paper we suggest to use satellite data and results of under-satellite synchronous measurements. The space image obtained from the satellite "Terra/MODIS" is represented in the form of two blocks of numerical matrices corresponding to the spectral radiance ( $W/(m^2 \cdot \mu m \cdot sr)$ ); an area of the underlying surface focused on pixels of the MODIS sensor; and the dimensionless parameter (reflection) equal to the ratio of the upward radiation to the radiation incident on the atmosphere top. The scanning angle varies between  $-55$  and  $+55^\circ$  from nadir.

The goal of atmospheric correction of the Earth's surface data obtained by remote sensing with the spaceborne devices (SD) is the estimation of the true magnitude of the underlying surface spectral radiance. Let  $B_{1\lambda}$  and  $B_{2\lambda}$  be the true radiance of an area of the underlying surface and the radiance of this area obtained from the SD sensor, respectively. The value of  $B_{1\lambda}$  is determined by the total natural irradiance and the albedo of this area assuming the Lambert reflection:

$$B_{1\lambda} = (E_{0\lambda} e^{-\tau_{\delta\lambda} m_{\theta}} \cos Z_{\theta}^0 + E_{\lambda H}) q_{\lambda} / \pi. \quad (1)$$

The value of  $B_{2\lambda}$  is the sum of the true radiance of the area of the underlying surface  $B_{1\lambda}$  attenuated in the atmosphere by  $e^{-\tau_{\delta\lambda} m}$  times, and the radiance of the upwelling total scattered radiation of the atmosphere  $\uparrow B_{\lambda}$ :

$$B_{2\lambda} = B_{1\lambda} e^{-\tau_{\delta\lambda} m} + \uparrow B_{\lambda} (\tau_{\delta\lambda}, \mu(\psi), Z_{\theta}^0, m), \quad (2)$$

where  $E_{0\lambda}$  is the extra-atmospheric spectral solar constant;  $\tau_{\delta\lambda}$  is the optical depth of the atmosphere extinction;  $m_{\theta}$  is the optical mass of the atmosphere in the direction to the Sun;  $m$  is the optical mass of the atmosphere in the direction of sensing from SD;  $Z_{\theta}^0$  is the zenith angle of the Sun;  $E_{\lambda H}$  is the component of natural spectral irradiance formed by the scattered light of the sky;  $q_{\lambda}$  is the spectral albedo of the underlying surface;  $\uparrow B_{\lambda}$  is the total radiance of the upwelling scattered radiation of the atmosphere in the direction of sensing from SD depending on the optical depth, phase function, zenith angle of the Sun, optical mass of the atmosphere in the direction of sensing, as well as the multiply scattered direct radiation, and the radiation reflected from the underlying surface in the atmosphere.

Let us consider the conditions, under which  $B_{1\lambda}$  and  $B_{2\lambda}$  can be equal.

Represent the true radiance of the underlying surface in the form

$$B_{1\lambda} = (B_{2\lambda} - \uparrow B_{\lambda}) / e^{-\tau_{\delta\lambda} m}.$$

If  $\uparrow B_{\lambda} = (1 - e^{-\tau_{\delta\lambda} m}) B_{2\lambda}$ , then  $B_{2\lambda} = B_{1\lambda}$ , and then: if  $\uparrow B_{\lambda} < (1 - e^{-\tau_{\delta\lambda} m}) B_{2\lambda}$ , then  $B_{2\lambda} < B_{1\lambda}$ , and at  $\uparrow B_{\lambda} > (1 - e^{-\tau_{\delta\lambda} m}) B_{2\lambda}$  we have  $B_{2\lambda} > B_{1\lambda}$ .

To determine the true magnitude of the spectral radiance of the underlying surface area from the remote sensing data (DRS), it is necessary to know  $e^{-\tau_{\delta\lambda}}$  and  $\uparrow B_{\lambda}$ . The value of the spectral optical depth of the atmosphere extinction  $\tau_{\delta\lambda}$  can be determined from synchronous ground-based measurements. The magnitude of the radiance of upwelling total scattered radiation of the atmosphere, in an ideal case, is equal

to the radiance of absolutely black part of the underlying surface sensed from SD. To determine  $\uparrow B_\lambda$ , one can use the fact that the spectral coefficient of the radiance of deep reservoirs with transparent water observed to nadir (out of the "solar track") is significantly less than the albedo of these reservoirs. The reservoir radiance observed to nadir is formed by the radiance of the water depth and the radiance of the scattered radiation reflected by the water reservoir surface from the zenith part of the sky.<sup>12</sup>

Spectral dependencies of the energetic radiance of different water reservoirs (Caspian Sea, lakes Balkhash, Issyk-Kul, Charyn) have been analyzed, as well as literature data on the radiance of the "ocean – atmosphere" system.<sup>12</sup> The results of the analysis have shown that the values of the spectral energetic radiance over Issyk-Kul and ocean are the closest.

To conduct atmospheric correction using RSD from MODIS, the spectral values of the radiance over Issyk-Kul on September 17, 2004 were used at sensing practically to nadir. To take into account the radiance of the water reservoir depth, the data on the spectral radiance of the central part of Black Sea were used obtained in the framework of the program "Interkosmos" from the Scientific-Research Vessel (SPV) *Professor Kolesnikov* of the Marine Hydrophysical Institute AS of Ukraine (the board height is 5 m).

The radiance spectra over Issyk-Kul obtained from MODIS on September 17, 2004 and from SRV *Professor Kolesnikov* (Black Sea) are shown in Fig. 1, as well as the obtained from these data radiance spectrum of the upwelling scattered radiation of the atmosphere  $\uparrow B_\lambda$  necessary for taking into account the background of the scattered radiation in the atmospheric correction. The data were obtained at  $Z_\theta^0$  of about 40°.

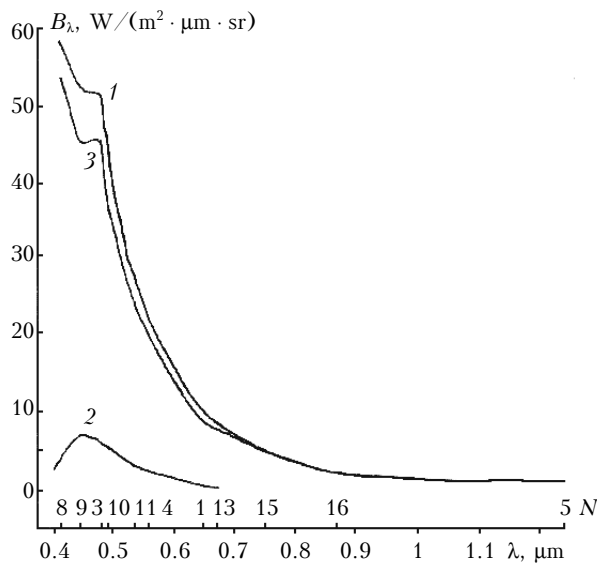


**Fig. 1.** Spectral energetic radiances: of upward radiation over Issyk-Kul, September 17, 2004 (1); of Black Sea (2); radiance of upward scattered radiation of the atmosphere (3).  $N$  is the number of spectral channels of the "Terra/MODIS" satellite.

Having the spectral energetic radiance of the upwelling scattered radiation of the atmosphere and the data of synchronous field measurements of the optical characteristics of the atmosphere on September 17, 2004, perform the atmospheric correction of two arbitrary selected areas of the underlying surface between lakes Balkhash and Issyk-Kul at the same scanning angles ( $\alpha = 25^\circ$ ).

The radiance spectra are shown in Fig. 2 in absolute energetic units of selected pixels before and after the atmospheric correction.

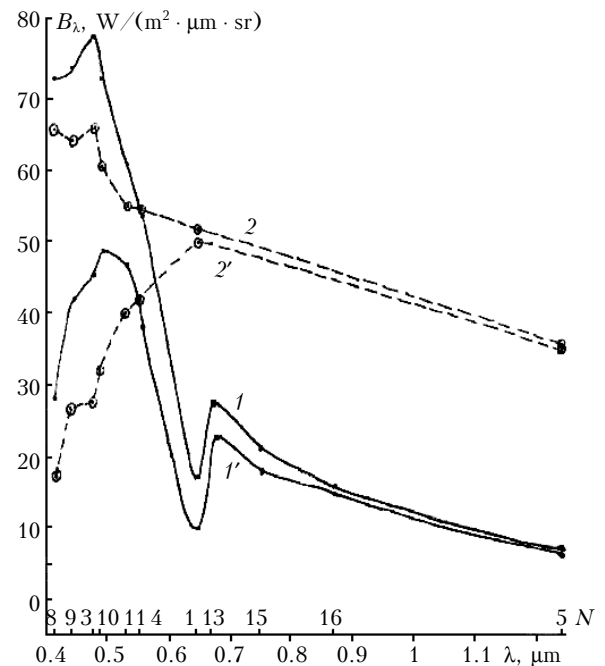


**Fig. 2.** Spectral energetic radiance on September 17, 2004 before (1 and 2) and after (1' and 2') atmospheric correction. Pixels 1 and 2 are arbitrary selected in the region between lakes Balkhash and Issyk-Kul.  $N$  is the number of spectral channels of the "Terra/MODIS" satellite.

As is seen in Fig. 2, atmospheric correction significantly changes the radiance spectrum of the areas of the underlying surface, obtained from SD, especially in the short-wave spectral range. The radiance of pixel 2 at  $\lambda = 0.412 \mu m$  decreases from 66 to 17.5  $W/(m^2 \cdot \mu m \cdot sr)$ .

To illustrate the spatial distribution of the spectral energetic radiance of the sensed part of the underlying surface before and after atmospheric correction, the pixel line is taken along the flight of SD at the same scanning angle  $\alpha = 25^\circ$  and  $\lambda = 0.412$  and  $0.479 \mu m$ . The part with varied underlying surface and mountains was selected.

The radiance distribution before and after atmospheric correction is shown in Figs. 3 and 4. The range of the radiance variation for the selected parts of the pixel line is between 0–70  $W/(m^2 \cdot \mu m \cdot sr)$  and 0–250  $W/(m^2 \cdot \mu m \cdot sr)$ .

It is seen that for less values of the radiance atmospheric correction leads to essential decrease of

the values of the radiance (Fig. 3a). The curves for mountain parts at great values of the radiance are crossed. It is caused by the fact that, as is shown above, at  $\hat{B}_\lambda = (1 - e^{-\tau_{0\lambda}^m})B_{2\lambda}$  the portions of the background scattered upwelling radiation and the attenuation of the true radiance magnitude of the pixel by the atmosphere become equal, i.e.,  $B_{2\lambda} = B_{1\lambda}$ . Analogous manner of variations of the spatial distribution of the radiance is also observed at  $\lambda = 0.479 \mu\text{m}$  (see Fig. 4). The scale is different. (Resolution at 0.412 and 0.479  $\mu\text{m}$  is different: 500×500 and 1000×1000 m, and the numbers of pixels along abscissa differ multiply).

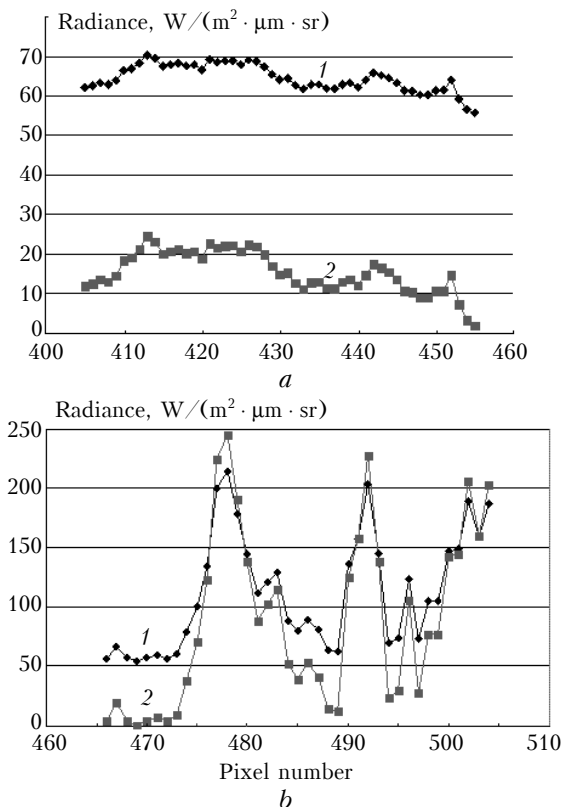


**Fig. 3.** Radiance distribution along the pixel line before (1) and after (2) atmospheric correction for the pixels: 405–455 (a); 465–505 (b) at  $\lambda = 0.412 \mu\text{m}$ , 8th channel.

The results of atmospheric correction are presented for two arbitrary selected pixels and at two wavelengths in the visible spectral range along the pixel line with maximum range of the radiance values recorded by the sensor of the satellite device.

To perform the atmospheric correction of space images of a finite area of the ground surface scanned by the sensor, it is necessary to use the spectral values of the atmospheric radiance phase function obtained from synchronous measurements taking into account the change of the zenith angle of the Sun for every pixel of the space image.

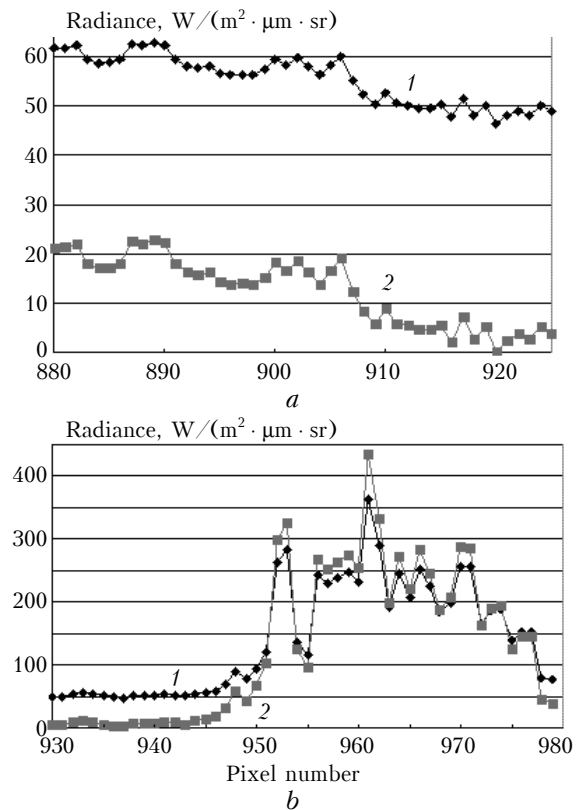


**Fig. 4.** Radiance distribution along the pixel line before (1) and after (2) atmospheric correction for the pixels: 880–925 (a); 930–980 (b) at  $\lambda = 0.479 \mu\text{m}$ , 3-d channel.

## References

1. U.M. Sultangazin, *J. of Inverse and ILL-Posed Problems* **9**, No. 6, 655–668 (2001).
2. T.A. Sushkevich, "About theory of optical transmission operator of the "atmosphere – Earth surface" system," Preprint, Institute of Applied Mathematics, Moscow (1999), 20 pp.
3. L.T. Matveev, *Atmospheric Physics* (Gidrometeoizdat, Leningrad, 1976), 477 pp.
4. E.V. Shalina, *Issled. Zemli iz Kosmosa*, No. 4, 59–65 (1995).
5. Yu.A. Volkov, I.N. Plakhina, and I.A. Repina, *Meteorol. Gidrol.*, No. 7, 14–21 (1999).
6. R.S. Fraser, R.A. Ferrare, Y.J. Kaufman, and S. Mattoo, *Int. J. Remote Sens.* **13**, No. 3, 541–557 (1992).
7. J. Dozier and J. Frew, *Remote Sens. Environ.* **11**, 191–205 (1981).
8. R.S. Fraser, R.A. Ferrare, Y.J. Kaufman, and S. Mattoo, *NASA Technical Memorandum*. 100751, 98 (1989).
9. Y.J. Kaufman and C. Sendra, *Int. J. Remote Sens.* **9**, No. 8, 1357–1381 (1988).
10. M. Putsay, *Int. J. Remote Sens.* **13**, No. 8, 1549–1558 (1992).
11. J.C. Roger, E. Vermote, and N. El Saleous, *Proc. SPIE* **2311**, 83–89 (1994).
12. V.A. Smerkolov, *Applied Atmospheric Optics* (Gidrometeoizdat, St. Petersburg, 1997), 373 pp.